



Published in final edited form as:

*Basic Res Cardiol.* ; 116(1): 35. doi:10.1007/s00395-021-00879-3.

## Mineralocorticoid receptor blockade normalizes coronary resistance in obese swine independent of functional alterations in $K_v$ channels

Adam G. Goodwill<sup>1</sup>, Hana E. Baker<sup>1</sup>, Gregory M. Dick<sup>2</sup>, Patricia E. McCallinhart<sup>3</sup>, Chastidy A. Bailey<sup>4,5</sup>, Scott M. Brown<sup>4,5</sup>, Joshua J. Man<sup>6,7</sup>, Darla L. Tharp<sup>4</sup>, Hannah E. Clark<sup>1</sup>, Bianca S. Blaettner<sup>1</sup>, Iris Z. Jaffe<sup>6</sup>, Douglas K. Bowles<sup>4,8</sup>, Aaron J. Trask<sup>3,9</sup>, Johnathan D. Tune<sup>2</sup>, Shawn B. Bender<sup>4,5,8,\*</sup>

<sup>1</sup>Department of Anatomy, Cell Biology, & Physiology, Indiana University School of Medicine, Indianapolis, IN, USA

<sup>2</sup>Department of Physiology and Anatomy, University of North Texas Health Science Center, Fort Worth, TX, USA

<sup>3</sup>Center for Cardiovascular Research, The Abigail Wexner Research Institute at Nationwide Children's Hospital, Columbus, OH, USA

<sup>4</sup>Department of Biomedical Sciences, University of Missouri, Columbia, MO, USA

<sup>5</sup>Research Service, Harry S. Truman Memorial Veterans Hospital, Columbia, Missouri, USA

<sup>6</sup>Molecular Cardiology Research Institute, Tufts Medical Center, Boston, MA, USA

<sup>7</sup>Graduate School of Biomedical Sciences, Tufts University School of Medicine, Boston, MA, USA

<sup>8</sup>Dalton Cardiovascular Research Center, University of Missouri, Columbia, MO, USA

<sup>9</sup>Department of Pediatrics, The Ohio State University College of Medicine, Columbus, OH, USA

### Abstract

Impaired coronary microvascular function (*e.g.*, reduced dilation and coronary flow reserve) predicts cardiac mortality in obesity, yet underlying mechanisms and potential therapeutic strategies remain poorly understood. Mineralocorticoid receptor (MR) antagonism improves coronary microvascular function in obese humans and animals. Whether MR blockade improves *in vivo* regulation of coronary flow, a process involving voltage-dependent  $K^+$  ( $K_v$ ) channel activation, or reduces coronary structural remodeling in obesity is unclear. Thus, the goals

\* **Correspondence:** Shawn Bender, PhD, Department of Biomedical Sciences, University of Missouri, E102 Veterinary Medicine Building, Columbia, MO 65211, benders@missouri.edu.

**Authors' Contributions:** AGG, JDT, and SBB conceived the study; AGG, PEM, DKB, AJT, JDT, and SBB designed the experiments; AGG, HEB, HEC, BSB, GMD, PEM, CAB, SMB, JJM, DLT, DKB, AJT, JDT, and SBB performed the experiments; All authors contributed to data analysis and interpretation; AGG, GMD, JDT, and SBB wrote the manuscript; All authors contributed to critical review and editing of the manuscript and approve the submitted version.

The authors declare that they have no conflict of interest.

Declarations

**Availability of Data and Material:** The datasets generated during and/or analyzed during the present study are available from the corresponding author on reasonable request.

This manuscript does not contain clinical studies or patient data.

of this investigation were to determine the effects of obesity on coronary responsiveness to reductions in arterial PO<sub>2</sub> and potential involvement of K<sub>v</sub> channels and whether the benefit of MR blockade involves improved coronary K<sub>v</sub> function or altered passive structural properties of the coronary microcirculation. Hypoxemia increased coronary blood flow similarly in lean and obese swine, however baseline coronary vascular resistance was significantly higher in obese swine. Inhibition of K<sub>v</sub> channels reduced coronary blood flow and augmented coronary resistance under baseline conditions in lean but not obese swine and had no impact on hypoxemic coronary vasodilation. Chronic MR inhibition in obese swine normalized baseline coronary resistance, did not influence hypoxemic coronary vasodilation, and did not restore coronary K<sub>v</sub> function (assessed *in vivo*, *ex vivo*, and via patch clamping). Lastly, MR blockade prevented obesity-associated coronary arteriolar stiffening independent of cardiac capillary density and changes in cardiac function. These data indicate that chronic MR inhibition prevents increased coronary resistance in obesity independent of K<sub>v</sub> channel function and is associated with mitigation of obesity-mediated coronary arteriolar stiffening.

### Keywords

aldosterone; obesity; hypoxemic vasodilation; potassium channels; vascular remodeling

---

## INTRODUCTION

The ability of the coronary circulation to maintain adequate oxygen delivery is essential to cardiac function and myocardial viability [15]. In obesity, coronary microvascular function is impaired and is associated with cardiac damage (*i.e.*, elevated troponin) and diastolic dysfunction [47, 48]. Consequently, coronary microvascular dysfunction is a powerful predictor of cardiac mortality in obese, diabetic patients [37] and increased risk of heart failure with preserved ejection fraction (HFpEF), especially for patients with combined cardiac diastolic dysfunction [48]. Indeed, the paradigm that co-morbidity-associated HFpEF may originate from coronary microvascular dysfunction has been proposed [40]. Critically, obesity-related HFpEF has recently been reported as a unique phenogroup within HFpEF populations having significantly elevated morbidity and mortality [12, 46] and unfortunately, there are currently no approved therapies for this highly prevalent condition. Thus, mechanistic understanding of obesity-associated coronary microvascular dysfunction is a promising avenue to novel treatment approaches for obesity-related cardiovascular disease.

One potential therapeutic strategy for coronary microvascular dysfunction in obesity focuses on the attenuation of chronic, maladaptive activation of aldosterone-sensitive mineralocorticoid receptors (MR). Recent studies, from our investigative team and others, indicate that systemic inhibition of MR signaling mitigates obesity-induced changes in microvascular vasomotor function, vascular and cardiac remodeling, and diastolic function in obese rodents [3, 9, 11, 14, 43]. Furthermore, the clinical relevance of MR antagonism is supported by evidence that MR blockade with eplerenone or spironolactone significantly increased coronary flow reserve (CFR) in obese humans with type 2 diabetes [4, 20, 27]. Whether these improvements in coronary vasomotor function are indicative of improvements

in local coronary control of vascular resistance *in vivo*, a process involving activation of voltage-gated  $K^+$  ( $K_V$ ) channels [21, 39], or attenuation of obesity-associated coronary structural remodeling remains unclear. Indeed, along with coronary arteriolar remodeling [28, 50], diminished coronary  $K_V$  function has been reported in obesity [6]. Importantly, aldosterone/MR signaling has recently been linked to the downregulation of vascular  $K^+$  channel activity and/or expression [16, 29] as well as to pathologic vascular remodeling in a variety of disease states [17]. Finally, much of the published work related to MR-dependent vascular dysfunction in co-morbid conditions has been performed in rodent models which are inherently limiting for studies examining mechanisms of coronary blood flow control *in vivo*. Thus, we propose to test the hypothesis that MR inhibition improves coronary function in a swine model of obesity, at least in part, by augmenting functional expression of coronary  $K_V$  channels and via normalization of coronary arteriolar structure.

## METHODS

All protocols were approved by the appropriate Institutional Animal Care and Use Committees in accordance with the *Guide for the Care and Use of Laboratory Animals* (NIH Pub. No. 85–23, Revised 2011) and the ethical standards laid down in the 1964 Declaration of Helsinki and its later amendments. Lean Ossabaw swine (n = 7; 4 females) were fed ~2,200 kcal/day of standard chow (5L80 Purina Test Diet) containing 18% kcal from protein, 71% kcal from complex carbohydrates, and 11% kcal from fat. Obese Ossabaw swine (n = 8; 4 females) were fed an excess calorie (~8,000 kcal/day), high-fat, high-fructose diet for ~16 weeks containing: 8% kcal from protein, 43% kcal from fat, 33% kcal from fructose, and 10% kcal from carbohydrates. An additional group of obese Ossabaw swine (n = 9; 4 females) received the MR antagonist spironolactone (25 mg/d, *po*) throughout the high-fat diet feeding period in a daily food snack. Lean and untreated obese swine received the same daily snack without spironolactone.

### Surgical preparation.

Swine were sedated with Telazol (tiletamin-zolazepam, 5 mg/kg, *sc*), xylazine (2.2 mg/kg, *sc*), and ketamine (3.0 mg/kg, *sc*). Following endotracheal intubation, anesthesia was maintained with morphine (3.0 mg/kg, *sc*) and  $\alpha$ -chloralose (100 mg/kg, *iv*). Following completion of the experimental protocol, hearts were fibrillated and excised in accordance with recommendation of the American Veterinary Medical Association Guide on Euthanasia (June 2020). Anesthetized swine were mechanically ventilated (Harvard respirator) with  $O_2$ -supplemented room air. Catheters were placed into the right femoral artery for systemic hemodynamic measurements and the right femoral vein for administration of supplemental anesthesia, heparin, and sodium bicarbonate. Blood samples for key phenotypic measurements (Table 1) were obtained immediately following placement of the venous catheter. Blood gas parameters were maintained within normal physiological limits throughout the protocol by periodic arterial blood gas analyses, appropriate adjustments to breathing rate, and bicarbonate supplementation as necessary. Ventilatory rate was maintained constant to limit/block arterial chemoreflex activation typically associated with hypoxemia-induced hyperventilation in free breathing animals [44]. A left lateral thoracotomy was performed to allow access to the heart after which

the left anterior descending coronary artery (LAD) was isolated and a perivascular flow transducer (Transonic Systems Inc.) placed around the vessel. A catheter was introduced into the coronary interventricular vein for coronary venous blood sampling and heparin was administered (bolus; 500 U/kg, iv). Hemodynamic parameters, coronary blood flow, and ECG were continuously measured throughout the entire protocol. All data were collected using IOX acquisition software (EMKA Technologies, Falls Church VA, USA).

### **In vivo experimental protocol.**

Following the surgical preparation and a ~15 min stabilization period, arterial and coronary venous blood samples were simultaneously collected under baseline (normoxic) conditions and analyzed with an Instrumentation Laboratories automatic blood gas analyzer (GEM Premier 4000). Hemodynamic parameters and arterial and coronary venous blood samples were obtained during graded coronary dilation elicited by hypoxemia. Specifically, PaO<sub>2</sub> was progressively diminished in four steps by supplementing ventilated air with increasing amounts of N<sub>2</sub> gas in order to reduce PaO<sub>2</sub> to approximately 65, 45, 35, and 25 mmHg. Once measurements and blood samples were collected at the most severe level of hypoxemia, the N<sub>2</sub> gas was turned off and PaO<sub>2</sub> returned to baseline, normoxic levels (typically within ~1–2 min). All swine then received the K<sub>v</sub> channel inhibitor 4-aminopyridine (4-AP, 0.3 mg/kg, iv) and the hypoxemia protocol repeated ~5 mins following 4-AP administration. Accordingly, each animal served as its own control and initial experiments revealed that hypoxemia-induced increases of coronary blood are repeatable with no tachyphylaxis (Online Resource 1). Myocardial oxygen consumption (MVO<sub>2</sub>; μl O<sub>2</sub>/min/g) and lactate uptake (μmol/min/g) were calculated using the Fick principle as [coronary blood flow x (arterial concentration – coronary venous concentration)]. Coronary vascular resistance was calculated from coronary blood flow and aortic blood pressure (*i.e.*, coronary perfusion pressure). Following the conclusion of the hypoxemia protocol, left ventricular (LV) function was assessed under normoxic conditions via a pressure-volume admittance catheter (Transonic Scisense, London, Ontario, Canada). The catheter was passed through a hemostatic control valve placed directly into the LV near the base via a transmural stab and secured with a purse string suture. Following *in vivo* experiments, swine were euthanized, the heart excised, coronary circulation immediately perfused with ice-cold physiological salt solution (PSS), and portions of the LV rapidly removed and placed in ice-cold PSS. Samples of LV were subsequently shipped overnight in ice-cold PSS to the University of Missouri and Nationwide Children's Hospital for *ex vivo* experiments, similar to previous studies [2, 5, 8, 50].

### **Wire myography.**

Subepicardial small coronary arteries were isolated, cleaned, and mounted in a wire myograph (Danish MyoTechnology) using 17μm stainless steel wire for assessment of vasomotor function, as previously described [1, 29]. Briefly, vessels were warmed to 37°C and equilibrated for 30–40 minutes with regular washing in Krebs-PSS containing (in mM): 119 NaCl, 4.7 KCl, 2.5 CaCl<sub>2</sub> 2H<sub>2</sub>O, 1.17 MgSO<sub>4</sub> 7H<sub>2</sub>O, 25 NaHCO<sub>3</sub>, 1.18 KH<sub>2</sub>PO<sub>4</sub>, 0.027 EDTA, and 5.5 glucose (pH 7.4; bubbled with 95% O<sub>2</sub>-5% CO<sub>2</sub>). Baseline tension was established using a normalization procedure [42], vessel viability was confirmed by exposure to 80 mM KCl-Krebs-PSS and, following washing, vasoconstrictor responses to

4-AP (3 mM) were assessed. Vasoconstrictor responses were normalized to vessel length and quantified as the change in measured tension in response to 4-AP.

### Pressure myography.

Coronary arterioles (<150  $\mu\text{m}$  internal diameter) were isolated from left ventricular tissue of the distal LAD, excised, mounted onto 2 glass microcannulas within a pressure myograph chamber (Living Systems, Burlington, VT), and equilibrated for 30 minutes under constant intraluminal pressure (50 mmHg) at 37°C in physiologic salt solution (PSS) (130 NaCl, 4 KCl, 1.2  $\text{MgSO}_4$ , 4  $\text{NaHCO}_3$ , 10 HEPES, 1.2  $\text{KH}_2\text{PO}_4$ , 5 glucose, and 2.5  $\text{CaCl}_2$  at pH 7.4). Measurements of coronary arteriolar structure and passive mechanical properties were assessed in  $\text{Ca}^{2+}$ -free PSS in the presence of 2mM EGTA and 100  $\mu\text{M}$  sodium nitroprusside. A passive pressure-diameter curve was generated by altering intraluminal pressure from a minimum of 0 mmHg to a maximum of 125 mmHg, and left and right wall thickness (WT) and internal diameters ( $D_i$ ) were recorded at each pressure using a video dimension analyzer (Living Systems Instrumentation, Burlington, VT). The following structural and mechanical parameters were calculated as previously described by us [28, 33, 50]:

*Circumferential Stress* ( $\sigma$ ) =  $(P \times D_i) / (2WT)$ , where P is pressure in dynes/cm<sup>2</sup>.

*Circumferential Strain* ( $\epsilon$ ) =  $(D_i - D_0) / D_0$ , where  $D_i$  is the internal diameter for a given intraluminal pressure and  $D_0$  is the original diameter measured at 0 mmHg of intraluminal pressure.

*Elastic modulus* (E) = stress ( $\sigma$ ) / strain ( $\epsilon$ ) is used to determine arterial stiffness. However, since the stress-strain relationship was non-linear we obtained the tangential or incremental elastic modulus ( $E_{\text{inc}}$ ), or simply the tangential slope of the stress-strain relationship at each incremental pressure ( $\sigma / \epsilon$ ).

### Patch clamp: smooth muscle cell (SMC) dissociation.

All electrophysiology experiments were performed using freshly dispersed arteriolar SMC. Coronary arterioles were placed in low- $\text{Ca}^{2+}$  (0.1 mM) physiological buffer containing 294 U/ml collagenase, 5 U/ml elastase, 2 mg/ml bovine serum albumin, 1 mg/ml soybean trypsin inhibitor, and 0.4 mg/ml DNase I. Cells were enzymatically dissociated by incubation in a 37 °C water bath for 60 min. The enzyme solution was then replaced with enzyme-free low- $\text{Ca}^{2+}$  solution and the arterioles dispersed with gentle trituration by micropipette for isolation of single SMCs. Smooth muscle cells were morphologically distinguishable from other cell types in the dispersion, such as endothelial cells and fibroblasts. Isolated cells were maintained in low- $\text{Ca}^{2+}$  solution at 4°C until use (0–6 h).

### Whole-cell voltage clamp.

Whole-cell  $\text{K}^+$  currents were obtained from single cells using standard whole-cell voltage clamp techniques, as used routinely [10, 22, 23]. Experiments were conducted under physiological  $\text{K}^+$  concentrations. Because membrane depolarization activates both  $\text{K}_v$  and large-conductance  $\text{Ca}^{2+}$ -dependent  $\text{K}^+$  ( $\text{BK}_{\text{Ca}}$ ) channels, we utilized low extracellular  $\text{Ca}^{2+}$  (0.1 mM) and 10 mM EGTA in the pipette to chelate intracellular  $\text{Ca}^{2+}$  and thereby

minimize the contribution of  $BK_{Ca}$  current to outward  $K^+$  current [52]. We also limited the depolarizing command pulses to +10 mV to minimize activation of  $BK_{Ca}$  channels [34]. The contribution of  $K_{ATP}$  channels to whole-cell  $K^+$  current was minimized by inclusion of 2 mM ATP in the pipette solution. Thus, these conditions allowed us to isolate  $K_v$  currents [22, 34, 52]. Cells were initially superfused with PSS containing (in mM): 138 NaCl, 5 KCl, 0.1  $CaCl_2$ , 1  $MgCl_2$ , 10 glucose, 20 HEPES, pH 7.4. Heat-polished glass pipettes (2–5 M $\Omega$ ) were filled with a solution containing (in mM): 120 KCl, 10 NaCl, 1  $MgCl_2$ , 10 EGTA, 10 HEPES, 2  $Na_2ATP$ , 0.5 Tris-GTP, pH 7.1 with KOH. Ionic currents were amplified with an Axopatch 200B patch-clamp amplifier (Axon Instruments). Currents were low-pass filtered with a cutoff frequency of 1000 Hz, digitized at 2.5 kHz and stored on computer. Cells were continuously perfused under gravity flow at room temperature (22–25°C). Sequential current-voltage (IV) relationships were obtained by 10 mV step depolarizations from –60 to +10mV from a holding potential of –80mV in PSS and PSS plus the  $K_v1$  blocker DPO-1 (10  $\mu$ M; Tocris). Data acquisition and analysis were accomplished using pClamp 9.0 software (Axon Instruments). Online leak subtraction was not performed.

### Immunofluorescence.

Capillary density was assessed in LV tissues that were fixed in 4% paraformaldehyde for 24–48 hrs and transferred to 70% EtOH until paraffin embedding and sectioning (5  $\mu$ m thickness). After deparaffinization and rehydration, antigen retrieval was performed using sodium citrate buffer (pH 6.0) and incubated with fish skin gelatin blocking serum (bovine serum albumin, cold water fish skin gelatin with tween) in PBS for 60 minutes at room temperature to suppress non-specific binding. Sections were stained with the endothelium marker fluorescein-conjugated isolectin (Vector Laboratories, Burlingame, CA) for 30 minutes at room temperature and the cell membrane marker rhodamine-conjugated wheat germ agglutinin (Vector Laboratories) for 30 minutes at room temperature. Nuclei were stained utilizing DAPI (ThermoFisher). Four randomly selected fields for each sample were imaged at 40X magnification. Images were coded after collection to allow for capillary counts and analysis by a blinded individual.

### Blood and plasma measures.

Following anesthesia, blood glucose and electrolytes were measured with an Instrumentation Laboratories automatic blood gas analyzer (GEM Premier 4000). Plasma insulin was measured by the Cornell University Animal Health Diagnostic Center. Total cholesterol and triglycerides were measured in serum by the University of Missouri Veterinary Medical Diagnostic Laboratory. Finally, plasma aldosterone was measured by competitive radioimmunoassay (Tecan, MG13051) in duplicate, according to manufacturer instructions.

### Statistical analyses.

Data are presented as individual data points or mean  $\pm$  SE and were analyzed using GraphPad Prism (GraphPad Software, San Diego, CA) and SigmaPlot (Systat Software, Inc., San Jose, CA). Artwork was generated in GraphPad Prism. Statistical comparisons for phenotypic, wire myography, and cardiac function data were performed by one-way analysis of variance (ANOVA). Coronary response variables (flow or resistance vs. arterial  $PO_2$ ) were compared with non-linear regression. Specifically, data were fit with one-phase

exponential curves and the extra sum-of-squares F test was used to determine whether one curve could adequately fit both groups. Coronary mechanical measurements were analyzed using a two-way repeated measures ANOVA. For all comparisons,  $P < 0.05$  was considered statistically significant. When significance was found with ANOVA, a Student-Newman-Keuls multiple comparison test was performed to identify differences.

## RESULTS

### Characterization of the swine obesity model.

Phenotypic data are shown in Table 1 for swine that were lean, obese, or obese and treated with spironolactone. As expected, the two groups of obese animals had body weights that were 24–26% higher than lean swine and similar heart weights thus the heart weight-to-body weight ratio was lower in the obese groups. Blood glucose was lower, plasma insulin and triglycerides were unchanged while total cholesterol was markedly increased in obese swine. Lastly, plasma aldosterone tended to be higher in the obese groups compared to lean swine ( $p = 0.06$ ) whereas plasma electrolytes ( $\text{Na}^+$  and  $\text{K}^+$ ) were unchanged. Assessment of systemic hemodynamics at baseline (*i.e.*, normoxia) and during graded hypoxemia revealed elevated mean aortic pressure in obese compared to lean swine (Figure 1a). Accordingly, obese swine had reduced heart rate but similar  $\text{MVO}_2$  compared to lean swine (Figures 1c and 1e). Treatment of obese swine with spironolactone resulted in reduced mean aortic pressure but no change in heart rate or  $\text{MVO}_2$  compared to untreated obese swine (Figures 1b, 1d, and 1f). Further, invasive assessment of LV hemodynamics under normoxic conditions revealed no impact of obesity on LV filling volume, stroke volume, ejection fraction, end-diastolic pressure, or LV diastolic time constant (Online Resource 2). Spironolactone treatment of obese swine did not significantly affect indices of cardiac function but tended to increase LV end-diastolic volume and stroke volume (Online Resource 2).

### Obesity increases coronary resistance but does not alter dilation to hypoxemia.

Coronary vascular responses to hypoxemia were measured in lean and obese swine (Figure 2). Average blood gas and hemodynamic parameters are provided in Online Resource 3. Under normoxic conditions, obese swine had reduced coronary blood flow (Figure 2a) corresponding to increased coronary resistance (Figure 2b), reduced coronary venous  $\text{PO}_2$ , and reduced myocardial lactate uptake (Online Resource 3) compared to lean swine. Arterial  $\text{PCO}_2$  was not changed during hypoxemia (Online Resource 3). As expected, graded hypoxemia reduced arterial  $\text{PO}_2$  and oxygen content with no change in hematocrit (Online Resource 3). Hypoxemia elicited profound increases in coronary blood flow as arterial  $\text{PO}_2$  dropped below 50 mmHg (Figure 2a) and this response was similar in lean and obese swine. In obese swine, hypoxemia resulted in myocardial lactate production (*i.e.*, reduced lactate uptake) relative to lean swine (Online Resource 3).

### Coronary $\text{K}_v$ channels are dysfunctional in obesity but do not contribute to hypoxemic dilation.

Inhibition of  $\text{K}_v$  channels *in vivo* with 4-AP in lean swine reduced baseline coronary blood flow (Figure 3a) and increased coronary resistance (Figure 3b) consistent with a role for

$K_V$  channels in normal coronary function. In contrast, 4-AP did not affect coronary blood flow (Figure 3c) or increase coronary resistance (Figure 3d) in obese swine. Notably, in both lean and obese swine,  $K_V$  blockade did not influence the degree of hypoxemic coronary vasodilation (Figure 3).

### **MR blockade prevents increased coronary resistance in obesity independent of $K_V$ channels.**

Treatment of obese swine with the MR antagonist spironolactone modestly increased coronary blood flow (Figure 4a) and significantly decreased baseline coronary resistance (Figure 4b) but did not affect coronary venous  $PO_2$  or myocardial lactate uptake (Online Resource 3) relative to untreated obese swine. Further, coronary hypoxic vasodilation was not impacted by spironolactone (Figure 4). Mechanistically, spironolactone treatment did not restore sensitivity to 4-AP *in vivo* in obese swine (Figure 4c and 4d). Further, isolated small coronary arteries from spironolactone-treated obese swine exhibited attenuated vasoconstriction to 4-AP similar to untreated obese swine (Figure 4e). Patch clamp studies revealed reduced whole cell  $K_V$  current in isolated coronary SMC from obese swine, compared to lean swine, that was not restored by spironolactone treatment (Figure 4f). Lastly, whole cell  $K_V$  currents were markedly reduced, and group differences abrogated, by treatment of SMCs with the  $K_V1$  family inhibitor DPO-1 (Figure 4f).

### **MR blockade prevents coronary arteriolar structural stiffening independent of capillary density in obesity.**

Assessment of cardiac capillary density revealed that although obese swine tended to have reduced capillary density compared to lean swine ( $p=0.09$ ), this was not statistically different and was not changed by spironolactone (Figure 5a). Accordingly, we further assessed coronary arteriolar biomechanics. Isolated, pressurized arterioles from the 3 treatment groups had similar passive internal diameters (Lean,  $111\pm 6\ \mu\text{m}$ ; Obese,  $137\pm 16\ \mu\text{m}$ ; Obese+Spiro,  $130\pm 12\ \mu\text{m}$ ; at 125 mmHg intraluminal pressure;  $p=0.36$ ) and wall thicknesses (Lean,  $12.3\pm 1.8\ \mu\text{m}$ ; Obese,  $13.2\pm 1.4\ \mu\text{m}$ ; Obese+Spiro,  $12.8\pm 0.8\ \mu\text{m}$  at 125 mmHg intraluminal pressure). Assessment of passive arteriolar biomechanics revealed a leftward shift of the stress-strain relationship (*i.e.*, stiffening) in obesity driven by reduced strain with no change in wall stress across the pressures examined (Figure 5b). Further, the incremental modulus of elasticity ( $E_{inc}$ ; an index of stiffness for non-linear elastic vessels) was increased in obesity at 125 mmHg. This impact of obesity was prevented by MR blockade as spironolactone-treated obese swine exhibited reduced strain, with no change in stress, and a reduced incremental modulus of elasticity compared to untreated obese swine (Figure 5c).

## **DISCUSSION**

Coronary microvascular resistance is tightly regulated to balance myocardial oxygen delivery with myocardial metabolism [15, 51]. This coupling between oxygen supply and demand is dependent on coronary  $K_V$  channels [6, 21, 39] that become dysfunctional in obesity [6]. Recent evidence indicates that MR blockade improves underlying coronary microvascular dysfunction in obese, diabetic patients [20, 27]. The purpose of this



investigation was to examine the extent to which MR-associated augmentation of microvascular responsiveness is mediated by improvements in the functional contribution of  $K_V$  channels to the control of coronary blood flow versus alterations in structural properties of the microcirculation. To that end, we demonstrate in a swine model of obesity that, 1) obesity decreases baseline coronary blood flow (increases resistance) but does not impair coronary dilation to hypoxemia in this model; 2) coronary  $K_V$  channels do not contribute to coronary microvascular resistance (flow) in obese swine and are not significant contributors to hypoxemia-induced coronary dilation; 3) MR blockade with spironolactone normalizes baseline coronary resistance in obese swine independent of  $K_V$  function; and 4) obesity-associated coronary arteriolar stiffening is prevented by chronic MR blockade. Together, these data reveal an independent role for MR activation and  $K_V$  channels in coronary microvascular impairment in obesity. Further, our results support that MR inhibition improves coronary microvascular resistance in obesity associated with prevention of adverse coronary arteriolar remodeling.

Our data confirm that resting coronary blood flow is reduced in obese swine owing to a pronounced increase in coronary vascular resistance, however, hypoxemia-induced coronary vasodilation is maintained in obese swine. The former observation is consistent with recent evidence of declining resting coronary perfusion with increasing body mass index in patients with and without diabetes [26]. Further, coronary venous  $PO_2$  was reduced in obese swine and this was associated with myocardial lactate production (*i.e.*, reduced lactate uptake) during hypoxemia indicative of impaired oxygen supply-demand balance in obesity. A primary aim of this study was to evaluate whether MR blockade prevents coronary microvascular dysfunction in obesity. To that end, our data demonstrate that MR blockade with a clinically relevant dose of spironolactone (25 mg/d) prevented increased baseline coronary resistance in obesity and did not impact the extent of coronary dilation to hypoxemia. In addition, despite reducing coronary resistance, spironolactone treatment did not change coronary venous  $PO_2$  or myocardial lactate uptake/production suggesting that decreased resistance was not associated with an improvement in the balance between coronary blood flow and cardiac metabolism. These data extend our previous findings that MR blockade restores coronary endothelial function in obese and diabetic rodents [3, 11] to demonstrate benefit of MR blockade on coronary resistance *in vivo* in the absence of diabetes. Critically, our data suggest that coronary microvascular dysfunction precedes changes in LV function in obesity, consistent with emerging narrative [40], but more detailed assessment of cardiac function is needed.

Recent evidence has established activation of  $K_V$  channels, specifically  $K_V1$  channels, as a primary regulator of coronary microvascular resistance at rest and in response to increases in  $MVO_2$  [21, 39]. Accordingly,  $K_V$  blockade *in vivo* and in isolated coronary small arteries induced pronounced coronary vasoconstriction in lean swine that was absent in obese non-diabetic swine, consistent with our previous report [6]. Our previous work indicates that obesity-associated  $K_V$  dysfunction involves downregulation of coronary  $K_V1.5$  channels [6]. Patch clamp experiments confirmed reduced  $K_V$  current in isolated coronary SMC from obese swine in the present study and, further, demonstrate that the majority of this current (>90%) is  $K_V1$ -dependent (*i.e.*, inhibited by DPO-1). Thus, coronary  $K_V1$  dysfunction is consistent with increased coronary resistance in obesity. Prior *in vitro* work

has implicated  $K_V1$  [49],  $K_V2$  [49], and  $K_V7$  [24] channels in hypoxia-induced vasodilation of porcine coronary vessels. Our *in vivo* data, however, indicate that  $K_V$  channels are not involved in coronary dilation to hypoxemia in lean or obese swine. To our knowledge, our data are the first to evaluate  $K_V$  involvement in hypoxemia-induced coronary vasodilation *in vivo*. Accordingly, future *in vivo* studies aimed at elucidating specific  $K^+$  channels involved in coronary dilation to hypoxemia are necessary as both ATP-sensitive ( $K_{ATP}$ ) and calcium-activated ( $K_{Ca}$ )  $K^+$  channels have also been implicated in this response [32, 35]. Notably, coronary arterioles from diabetic patients were reported to have impaired dilation to hypoxia involving  $K_{ATP}$  dysfunction [35]. Our data further demonstrate that the improvement of coronary resistance by MR blockade with spironolactone in obese swine does not involve improved coronary  $K_V$  function. Indeed,  $K_V$  blockade did not induce coronary vasoconstriction *in vivo* or in isolated coronary arteries in obese swine treated with spironolactone consistent with no improvement of  $K_V$  current in coronary SMC isolated from these swine. Thus, alternative mechanisms of coronary tone regulation or coronary structural alterations account for the benefit of MR blockade on coronary resistance in obesity.

Previous reports have demonstrated that coronary arterioles from *db/db* mice and Ossabaw swine with metabolic syndrome undergo inward hypertrophic remodeling associated with reduced vessel stiffness [28, 50]. Interestingly, our data reveal increased stiffness (*i.e.*, reduced distensibility) of coronary arterioles from obese Ossabaw swine independent of changes in luminal diameter or wall thickness. Reasons for the discrepant arteriolar phenotypes between this and previous work in the Ossabaw swine are unclear but may be related to length of experimental diet feeding (4 vs 6 months), diet composition (33% vs 19% fructose), or differences in underlying glucose/insulin sensitivity in the current study [50]. Regardless, our data suggest that obesity-associated arteriolar stiffening in the present study likely involves a combination of extracellular matrix (ECM) and intrinsic cell mechanical alterations that warrant further examination. Further, our data reveal that spironolactone prevents coronary arteriolar stiffening and the increase of  $E_{inc}$  in obese swine. To our knowledge, these are the first data exploring the impact of MR blockade on coronary microvascular biomechanics in obesity and are consistent with accumulating evidence for a role of inappropriate MR signaling in vascular stiffening in co-morbid conditions [7, 11, 31]. Notably, MR signaling is closely associated with vascular ECM regulation [7] and MR blockade is associated with reduced biomarkers of collagen metabolism in patients at risk of developing heart failure [19]. The extent to which these changes might reflect alterations in coronary vascular stiffness remains to be determined. Nonetheless, our data indicate that attenuation of MR-dependent changes in coronary extracellular matrix composition/regulation contributes, at least in part, to the normalization of arteriolar distensibility by spironolactone in obesity. Overall, in the absence of restored  $K_V$  function by spironolactone in obese swine, these data support a role for MR-dependent arteriolar stiffening underlying increased coronary resistance in obesity.

It is important to acknowledge several limitations of the present study. First, treatment groups in this study included a balance of both male and female swine. Sex differences in the prevalence and mechanisms of obesity-associated microvascular dysfunction have been reported for coronary and peripheral vascular beds [36]. In addition, sex specificity of MR-

dependent mechanisms of vascular dysfunction in co-morbid conditions have been reported, mainly regarding endothelial impacts of MR signaling [13, 36]. Whether obesity-associated and MR-dependent alterations in SMC function, particularly involving  $K_V$  channels, are sex specific remains to be determined as the present study is insufficiently powered to detect sex differences. In addition, a group of lean swine treated with spironolactone was not included in this study. Available evidence indicates that blockade or genetic deletion of MR has little impact on vascular function in lean animals or patients. Specifically, spironolactone or endothelial cell-specific MR deletion did not alter vascular function nor did smooth muscle-specific MR deletion alter CFR in lean mice [13, 14, 30, 43]. Spironolactone also did not improve outcomes in HFpEF patients with a body mass index less than 30 (*i.e.*, non-obese) or normal waist circumference [18]. Further, our data do not suggest significant activation of the chemoreceptor reflex in response to reduced arterial  $PO_2$ . We believe this is likely due to a mitigation of this reflex by anesthesia. Finally, while plasma aldosterone tended to be increased in obese swine in this study, the mechanisms of MR activation in obesity remain unclear. Indeed, in addition to activation by aldosterone, activation of MR in a ligand-independent manner by angiotensin II [25] and by Rac1 GTPase in response to oxidative stress [38] has been reported as well as activation by cortisol and other serum factors. Accordingly, future work is needed to clarify obesity-associated mechanisms of MR activation.

Despite these limitations, our data have important implications regarding mechanisms of coronary microvascular dysfunction in obesity as well as the relationship between coronary dysfunction and ultimate cardiac outcomes. First, our data reveal MR-dependent mechanisms of coronary microvascular dysfunction largely independent of the overall regulation of microvascular responsiveness to graded reductions of oxygen supply in obesity. In this context, it should be noted that  $MVO_2$  was not changed during hypoxemia. Therefore, whether MR blockade improves coronary dilation in response to increased cardiac metabolism warrants further examination. Interestingly, however, the decrease in baseline coronary resistance following spironolactone treatment did not substantially improve myocardial oxygen supply-demand balance as coronary venous  $PO_2$  and myocardial lactate uptake remain decreased relative to lean swine. In light of this, our data in a translationally relevant large animal model are insightful in suggesting potential coronary blood flow-independent mechanisms underlying the benefit of spironolactone to reduce hospitalization for heart failure in obese patients enrolled from the Americas in the recent Treatment of Preserved Cardiac Function Heart Failure with an Aldosterone Antagonist (TOPCAT) trial [41]. Specifically, our data suggest improved LV filling (*i.e.*, trend for increased LV end diastolic volume) in obese swine treated with spironolactone, consistent with prior work in obese mice [9]. Thus, myocardial contractile function or structure may be altered by MR blockade in obesity consistent with the prevention of arteriolar stiffening by spironolactone and warrants further study. Importantly, the benefit of MR blockade to improve outcomes in 'TOPCAT-Americas' increased linearly with increasing BMI highlighting the role of obesity-associated MR activation [18]. Further work in cell-specific MR knockout models is necessary to fully delineate vascular MR-dependent mechanisms of cardiac dysfunction in obesity related to and beyond the control of coronary blood flow. Lastly, a recent bimodal distribution paradigm of coronary microvascular dysfunction has been proposed

in obesity/diabetes such that early coronary functional defects are followed by progression to coronary structural remodeling [45]. That MR blockade prevented obesity-associated coronary arteriolar stiffening in obese swine highlights the potential for MR blockade to attenuate or prevent the progression of coronary dysfunction in obesity.

In summary, our data address an important gap in the understanding of obesity-associated coronary microvascular dysfunction and the potential therapeutic impact of MR blockade. These data extend previous clinical and preclinical work to a large animal model of obesity to reveal novel mechanisms for the benefits of MR blockade on coronary microvascular function and structure. Overall, this study supports the emerging rationale for the use of MR antagonists to improve or preserve coronary microvascular, and ultimately cardiac, function in obesity.

## Supplementary Material

Refer to Web version on PubMed Central for supplementary material.

## Acknowledgements:

The authors are grateful to Clayton Douglas, Dana Weir, Christian Aragonz, and Margot Ruff.

**Funding:** This work was supported by National Institutes of Health grants R01 HL136386 (SBB), R00 HL116769 (AJT), R21 EB026518 (AJT), S10 OD023438 (AJT), R01 HL095590 (IZJ), U42 OD011140 to the National Swine Resource and Research Center (strain RRID- NSRRC:0008), The Abigail Wexner Research Institute at Nationwide Children's Hospital (AJT), and the use of facilities and resources at the Harry S. Truman Memorial Veterans' Hospital in Columbia, MO.

## REFERENCES

1. Barrett Mueller K, Bender SB, Hong K, Yang Y, Aronovitz M, Jaisser F, Hill MA, Jaffe IZ (2015) Endothelial Mineralocorticoid Receptors Differentially Contribute to Coronary and Mesenteric Vascular Function Without Modulating Blood Pressure. *Hypertension* 66:988–997 doi:10.1161/hypertensionaha.115.06172 [PubMed: 26351033]
2. Bender SB, Berwick ZC, Laughlin MH, Tune JD (2011) Functional contribution of P2Y1 receptors to the control of coronary blood flow. *J Appl Physiol* 111:1744–1750 doi:10.1152/jappphysiol.00946.2011 [PubMed: 21940850]
3. Bender SB, DeMarco VG, Padilla J, Jenkins NT, Habibi J, Garro M, Pulakat L, Aroor AR, Jaffe IZ, Sowers JR (2015) Mineralocorticoid Receptor Antagonism Treats Obesity-Associated Cardiac Diastolic Dysfunction. *Hypertension* 65:1082–1088 doi:10.1161/hypertensionaha.114.04912 [PubMed: 25712719]
4. Bender SB, Jia G, Sowers JR (2015) Mineralocorticoid receptors: an appealing target to treat coronary microvascular dysfunction in diabetes. *Diabetes* 64:3–5 doi:10.2337/db14-1425 [PubMed: 25538279]
5. Bender SB, Tune JD, Borbouse L, Long X, Sturek M, Laughlin MH (2009) Altered mechanism of adenosine-induced coronary arteriolar dilation in early-stage metabolic syndrome. *Exp Biol Med* (Maywood) 234:683–692 doi:10.3181/0812-RM-350 [PubMed: 19307464]
6. Berwick ZC, Dick GM, Moberly SP, Kohr MC, Sturek M, Tune JD (2012) Contribution of voltage-dependent K<sup>+</sup> channels to metabolic control of coronary blood flow. *J Mol Cell Cardiol* 52:912–919 doi:10.1016/j.yjmcc.2011.07.004 [PubMed: 21771599]
7. Biwer LA, Wallingford MC, Jaffe IZ (2019) Vascular Mineralocorticoid Receptor: Evolutionary Mediator of Wound Healing Turned Harmful by Our Modern Lifestyle. *Am J Hypertens* 32:123–134 doi:10.1093/ajh/hpy158 [PubMed: 30380007]

8. Borbouse L, Dick GM, Asano S, Bender SB, Dincer UD, Payne GA, Neeb ZP, Bratz IN, Sturek M, Tune JD (2009) Impaired function of coronary BK(Ca) channels in metabolic syndrome. *Am J Physiol Heart Circ Physiol* 297:H1629–1637 doi:10.1152/ajpheart.00466.2009 [PubMed: 19749164]
9. Bostick B, Habibi J, DeMarco VG, Jia G, Domeier TL, Lambert MD, Aroor AR, Nistala R, Bender SB, Garro M, Hayden MR, Ma L, Manrique C, Sowers JR (2015) Mineralocorticoid receptor blockade prevents Western diet-induced diastolic dysfunction in female mice. *Am J Physiol Heart Circ Physiol* 308:H1126–1135 doi:10.1152/ajpheart.00898.2014 [PubMed: 25747754]
10. Bowles DK, Laughlin MH, Sturek M (1998) Exercise training increases K<sup>+</sup> channel contribution to regulation of coronary arterial tone. *J Appl Physiol* 84:1225–1233 doi: 10.1152/jappl.1998.84.4.1225 [PubMed: 9516188]
11. Brown SM, Meuth AI, Davis JW, Rector RS, Bender SB (2018) Mineralocorticoid receptor antagonism reverses diabetes-related coronary vasodilator dysfunction: A unique vascular transcriptomic signature. *Pharmacol Res* 134:100–108 doi:10.1016/j.phrs.2018.06.002 [PubMed: 29870805]
12. Cohen JB, Schrauben SJ, Zhao L, Basso MD, Cvijic ME, Li Z, Yarde M, Wang Z, Bhattacharya PT, Chirinos DA, Prenner S, Zamani P, Seiffert DA, Car BD, Gordon DA, Margulies K, Cappola T, Chirinos JA (2020) Clinical Phenogroups in Heart Failure With Preserved Ejection Fraction: Detailed Phenotypes, Prognosis, and Response to Spironolactone. *JACC Heart Fail* 8:172–184 doi:10.1016/j.jchf.2019.09.009 [PubMed: 31926856]
13. Davel AP, Lu Q, Moss ME, Rao S, Anwar IJ, DuPont JJ, Jaffe IZ (2018) Sex-Specific Mechanisms of Resistance Vessel Endothelial Dysfunction Induced by Cardiometabolic Risk Factors. *J Am Heart Assoc* 7 doi:10.1161/jaha.117.007675
14. DeMarco VG, Habibi J, Jia G, Aroor AR, Ramirez-Perez FI, Martinez-Lemus LA, Bender SB, Garro M, Hayden MR, Sun Z, Meiningner GA, Manrique C, Whaley-Connell A, Sowers JR (2015) Low-Dose Mineralocorticoid Receptor Blockade Prevents Western Diet-Induced Arterial Stiffening in Female Mice. *Hypertension* 66:99–107 doi:10.1161/hypertensionaha.115.05674 [PubMed: 26015449]
15. Duncker DJ, Bache RJ (2008) Regulation of coronary blood flow during exercise. *Physiol Rev* 88:1009–1086 doi: 10.1152/physrev.00045.2006 [PubMed: 18626066]
16. DuPont JJ, Hill MA, Bender SB, Jaisser F, Jaffe IZ (2014) Aldosterone and Vascular Mineralocorticoid Receptors: Regulators of Ion Channels Beyond the Kidney. *Hypertension* 63:632–637 doi:10.1161/hypertensionaha.113.01273 [PubMed: 24379184]
17. DuPont JJ, Jaffe IZ (2017) 30 YEARS OF THE MINERALOCORTICOID RECEPTOR: The role of the mineralocorticoid receptor in the vasculature. *J Endocrinol* 234:T67–T82 doi:10.1530/joe-17-0009 [PubMed: 28634267]
18. Elkholey K, Papadimitriou L, Butler J, Thadani U, Stavrakis S (2021) Effect of Obesity on Response to Spironolactone in Patients with Heart Failure with Preserved Ejection Fraction. *Am J Cardiol* doi:10.1016/j.amjcard.2021.01.018
19. Ferreira JP, Verdonschot J, Wang P, Pizard A, Collier T, Ahmed FZ, Brunner-La-Rocca H-P, Clark AL, Cosmi F, Cuthbert J, Díez J, Edelmann F, Gierd N, González A, Grojean S, Hazebroek M, Khan J, Latini R, Mamas MA, Mariottoni B, Mujaj B, Pellicori P, Petutschnigg J, Pieske B, Rossignol P, Rouet P, Staessen JA, Cleland JGF, Heymans S, Zannad F (2021) Proteomic and Mechanistic Analysis of Spironolactone in Patients at Risk for HF. *JACC Heart Fail* doi:10.1016/j.jchf.2020.11.010
20. Garg R, Rao AD, Baimas-George M, Hurwitz S, Foster C, Shah RV, Jerosch-Herold M, Kwong RY, Di Carli MF, Adler GK (2015) Mineralocorticoid receptor blockade improves coronary microvascular function in individuals with type 2 diabetes. *Diabetes* 64:236–242 doi:10.2337/db14-0670 [PubMed: 25125488]
21. Goodwill AG, Noblet JN, Sassoon D, Fu L, Kassab GS, Schepers L, Herring BP, Rottgen TS, Tune JD, Dick GM (2016) Critical contribution of KV1 channels to the regulation of coronary blood flow. *Basic Res Cardiol* 111:1–13 doi:10.1007/s00395-016-0575-0 [PubMed: 26597728]
22. Heaps CL, Bowles DK (2002) Gender-specific K(+) -channel contribution to adenosine-induced relaxation in coronary arterioles. *J Appl Physiol* 92:550–558 doi: 10.1152/japplphysiol.00566.2001 [PubMed: 11796663]

23. Heaps CL, Tharp DL, Bowles DK (2005) Hypercholesterolemia abolishes voltage-dependent K<sup>+</sup> channel contribution to adenosine-mediated relaxation in porcine coronary arterioles. *Am J Physiol Heart Circ Physiol* 288:H568–H576 doi: 10.1152/ajpheart.00157.2004 [PubMed: 15458946]
24. Hedegaard ER, Nielsen BD, Kun A, Hughes AD, Krøigaard C, Mogensen S, Matchkov VV, Frøbert O, Simonsen U (2014) KV7 channels are involved in hypoxia-induced vasodilatation of porcine coronary arteries. *Br J Pharmacol* 171:69–82 doi:10.1111/bph.12424 [PubMed: 24111896]
25. Jaffe IZ, Mendelsohn ME (2005) Angiotensin II and aldosterone regulate gene transcription via functional mineralocorticoid receptors in human coronary artery smooth muscle cells. *Circ Res* 96:643–650 doi:10.1161/01.RES.0000159937.05502.d1 [PubMed: 15718497]
26. Jiang L, Shi K, Guo Y-k, Ren Y, Li Z-l, Xia C-c, Li L, Liu X, Xie L-j, Gao Y, Shen M-t, Deng M-y, Yang Z-g (2020) The additive effects of obesity on myocardial microcirculation in diabetic individuals: a cardiac magnetic resonance first-pass perfusion study. *Cardiovasc Diabetol* 19:52 doi:10.1186/s12933-020-01028-1 [PubMed: 32375795]
27. Joffe HV, Kwong RY, Gerhard-Herman MD, Rice C, Feldman K, Adler GK (2007) Beneficial effects of eplerenone versus hydrochlorothiazide on coronary circulatory function in patients with diabetes mellitus. *J Clin Endocrinol Metab* 92:2552–2558 doi:10.1210/jc.2007-0393 [PubMed: 17488800]
28. Katz PS, Trask AJ, Souza-Smith FM, Hutchinson KR, Galantowicz ML, Lord KC, Stewart JA Jr, Cismowski MJ, Varner KJ, Lucchesi PA (2011) Coronary arterioles in type 2 diabetic (db/db) mice undergo a distinct pattern of remodeling associated with decreased vessel stiffness. *Basic Res Cardiol* 106:1123–1134 doi:10.1007/s00395-011-0201-0 [PubMed: 21744279]
29. Khan M, Meuth AI, Brown SM, Chandrasekar B, Bowles DK, Bender SB (2019) Aldosterone impairs coronary adenosine-mediated vasodilation via reduced functional expression of Ca<sup>2+</sup>-activated K<sup>+</sup> channels. *Am J Physiol Heart Circ Physiol* 317:H357–H363 doi:10.1152/ajpheart.00081.2019 [PubMed: 31199187]
30. Kim SK, Biwer LA, Moss ME, Man JJ, Aronovitz MJ, Martin GL, Carrillo-Salinas FJ, Salvador AM, Alcaide P, Jaffe IZ (2021) Mineralocorticoid Receptor in Smooth Muscle Contributes to Pressure Overload-Induced Heart Failure. *Circ Heart Fail* 14:e007279 doi:10.1161/circheartfailure.120.007279 [PubMed: 33517669]
31. Kim SK, McCurley AT, DuPont JJ, Aronovitz M, Moss ME, Stillman IE, Karumanchi SA, Christou DD, Jaffe IZ (2018) Smooth Muscle Cell-Mineralocorticoid Receptor as a Mediator of Cardiovascular Stiffness With Aging. *Hypertension* 71:609–621 doi:10.1161/hypertensionaha.117.10437 [PubMed: 29463624]
32. Liu Q, Flavahan NA (1997) Hypoxic dilatation of porcine small coronary arteries: role of endothelium and KATP-channels. *Br J Pharmacol* 120:728–734 doi:10.1038/sj.bjp.0700939 [PubMed: 9051315]
33. McCallinhardt PE, Sunyecz IL, Trask AJ (2018) Coronary Microvascular Remodeling in Type 2 Diabetes: Synonymous With Early Aging? *Front Physiol* 9 doi:10.3389/fphys.2018.01463 [PubMed: 29467662]
34. Miller AL, Morales E, Leblanc NR, Cole WC (1993) Metabolic inhibition enhances Ca<sup>2+</sup>-activated K<sup>+</sup> current in smooth muscle cells of rabbit portal vein. *Am J Physiol* 265:H2184–H2195 doi: 10.1152/ajpheart.1993.265.6.H2184 [PubMed: 8285258]
35. Miura H, Wachtel RE, Loberiza FR Jr, Saito T, Miura M, Nicolosi AC, Gutterman DD (2003) Diabetes mellitus impairs vasodilation to hypoxia in human coronary arterioles: reduced activity of ATP-sensitive potassium channels. *Circ Res* 92:151–158 doi: 10.1161/01.res.0000052671.53256.49 [PubMed: 12574142]
36. Moss ME, Carvajal B, Jaffe IZ (2019) The endothelial mineralocorticoid receptor: Contributions to sex differences in cardiovascular disease. *Pharmacol Ther* 203:107387 doi:10.1016/j.pharmthera.2019.06.009 [PubMed: 31271793]
37. Murthy VL, Naya M, Foster CR, Gaber M, Hainer J, Klein J, Dorbala S, Blankstein R, Di Carli MF (2012) Association between coronary vascular dysfunction and cardiac mortality in patients with and without diabetes mellitus. *Circulation* 126:1858–1868 doi:10.1161/CIRCULATIONAHA.112.120402 [PubMed: 22919001]

38. Nagase M, Ayuzawa N, Kawarazaki W, Ishizawa K, Ueda K, Yoshida S, Fujita T (2012) Oxidative Stress Causes Mineralocorticoid Receptor Activation in Rat Cardiomyocytes. *Hypertension* 59:500–506 doi:doi:10.1161/HYPERTENSIONAHA.111.185520 [PubMed: 22232135]
39. Ohanyan V, Yin L, Bardakjian R, Kolz C, Enrick M, Hakobyan T, Kmetz J, Bratz I, Luli J, Nagane M, Khan N, Hou H, Kuppusamy P, Graham J, Fu FK, Janota D, Oyewumi MO, Logan S, Lindner JR, Chilian WM (2015) Requisite Role of Kv1.5 Channels in Coronary Metabolic Dilation. *Circ Res* 117:612–621 doi:10.1161/circresaha.115.306642 [PubMed: 26224794]
40. Paulus WJ, Tschöpe C (2013) A Novel Paradigm for Heart Failure With Preserved Ejection Fraction: Comorbidities Drive Myocardial Dysfunction and Remodeling Through Coronary Microvascular Endothelial Inflammation. *J Am Coll Cardiol* 62:263–271 doi:10.1016/j.jacc.2013.02.092 [PubMed: 23684677]
41. Pfeffer MA, Claggett B, Assmann SF, Boineau R, Anand IS, Clausell N, Desai AS, Diaz R, Fleg JL, Gordeev I, Heitner JF, Lewis EF, O'Meara E, Rouleau J-L, Probstfield JL, Shaburishvili T, Shah SJ, Solomon SD, Sweitzer NK, McKinlay SM, Pitt B (2015) Regional Variation in Patients and Outcomes in the Treatment of Preserved Cardiac Function Heart Failure With an Aldosterone Antagonist (TOPCAT) Trial. *Circulation* 131:34–42 doi:10.1161/circulationaha.114.013255 [PubMed: 25406305]
42. Richard V, Kaeffer N, Tron C, Thuillez C (1994) Ischemic preconditioning protects against coronary endothelial dysfunction induced by ischemia and reperfusion. *Circulation* 89:1254–1261 doi:10.1161/01.cir.89.3.1254 [PubMed: 8124814]
43. Schafer N, Lohmann C, Winnik S, van Tits LJ, Miranda MX, Vergopoulos A, Ruschitzka F, Nussberger J, Berger S, Luscher TF, Verrey F, Matter CM (2013) Endothelial mineralocorticoid receptor activation mediates endothelial dysfunction in diet-induced obesity. *Eur Heart J* 34:3515–3524 doi:10.1093/eurheartj/ehd095 [PubMed: 23594590]
44. Schultz HD, Li YL, Ding Y (2007) Arterial Chemoreceptors and Sympathetic Nerve Activity. *Hypertension* 50:6–13 doi:doi:10.1161/HYPERTENSIONAHA.106.076083 [PubMed: 17502495]
45. Sezer M, Kocaaga M, Aslanger E, Atici A, Demirkiran A, Bugra Z, Umman S, Umman B (2016) Bimodal Pattern of Coronary Microvascular Involvement in Diabetes Mellitus. *J Am Heart Assoc* 5:e003995 doi:doi:10.1161/JAHA.116.003995 [PubMed: 27930353]
46. Shah SJ, Katz DH, Selvaraj S, Burke MA, Yancy CW, Gheorghide M, Bonow RO, Huang C-C, Deo RC (2015) Phenomapping for Novel Classification of Heart Failure With Preserved Ejection Fraction. *Circulation* 131:269–279 doi:doi:10.1161/CIRCULATIONAHA.114.010637 [PubMed: 25398313]
47. Taqueti VR, Everett BM, Murthy VL, Gaber M, Foster CR, Hainer J, Blankstein R, Dorbala S, Di Carli MF (2015) Interaction of Impaired Coronary Flow Reserve and Cardiomyocyte Injury on Adverse Cardiovascular Outcomes in Patients Without Overt Coronary Artery Disease. *Circulation* 131:528–535 doi:10.1161/circulationaha.114.009716 [PubMed: 25480813]
48. Taqueti VR, Solomon SD, Shah AM, Desai AS, Groarke JD, Osborne MT, Hainer J, Bibbo CF, Dorbala S, Blankstein R, Di Carli MF (2018) Coronary microvascular dysfunction and future risk of heart failure with preserved ejection fraction. *Eur Heart J* 39:840–849 doi:10.1093/eurheartj/ehx721 [PubMed: 29293969]
49. Thorne GD, Conforti L, Paul RJ (2002) Hypoxic vasorelaxation inhibition by organ culture correlates with loss of Kv channels but not Ca<sup>2+</sup> channels. *Am J Physiol Heart Circ Physiol* 283:H247–H253 doi:10.1152/ajpheart.00569.2001 [PubMed: 12063297]
50. Trask AJ, Katz PS, Kelly AP, Galantowicz ML, Cismowski MJ, West TA, Neeb ZP, Berwick ZC, Goodwill AG, Alloosh M, Tune JD, Sturek M, Lucchesi PA (2012) Dynamic micro- and macrovascular remodeling in coronary circulation of obese Ossabaw pigs with metabolic syndrome. *J Appl Physiol* 113:1128–1140 doi:10.1152/jappphysiol.00604.2012 [PubMed: 22837170]
51. Tune JD, Goodwill AG, Kiel AM, Baker HE, Bender SB, Merkus D, Duncker DJ (2020) Disentangling the Gordian knot of local metabolic control of coronary blood flow. *Am J Physiol Heart Circ Physiol* 318:H11–H24 doi:10.1152/ajpheart.00325.2019 [PubMed: 31702972]
52. Volk KA, Matsuda JJ, Shibata EF (1991) A voltage-dependent potassium current in rabbit coronary artery smooth muscle cells. *J Physiol (Lond)* 439:751–768 doi: 10.1113/jphysiol.1991.sp018691 [PubMed: 1910087]

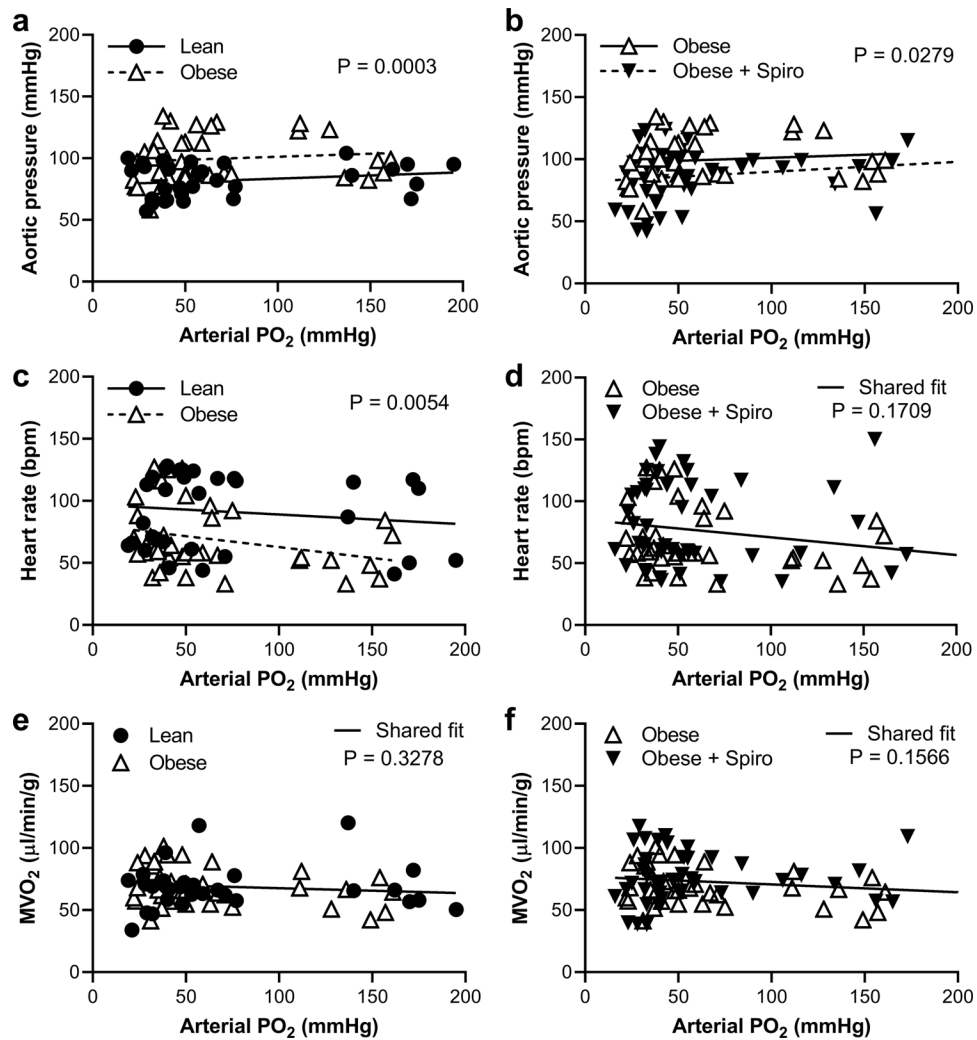


**Fig. 1. Obese swine have higher aortic blood pressure compared to lean swine that was reduced by MR inhibition.**

Lean and obese untreated swine (a, c, e) and obese untreated and spironolactone (Spiro)-treated swine (b, d, f) were compared during graded reductions of arterial  $PO_2$  to induce hypoxemia while measuring aortic pressure (a, b), heart rate (c, d), and myocardial oxygen consumption ( $MVO_2$ ; e, f). Individual data points shown,  $n=7-9$  per group, significance indicated by panel based on non-linear regression



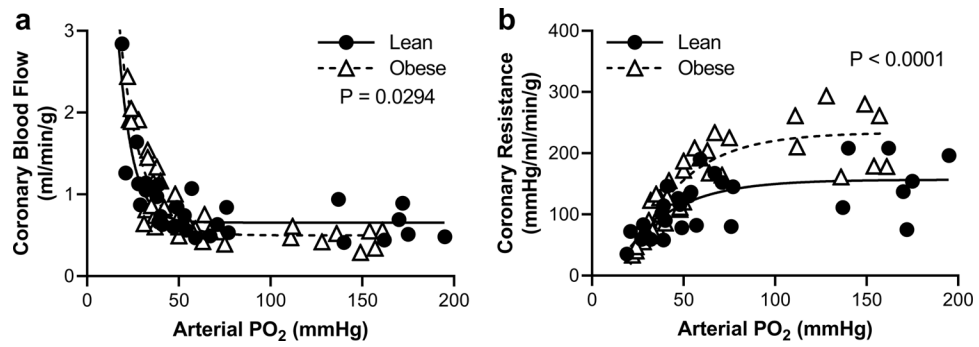


**Fig. 2. Obesity increases coronary vascular resistance but does not limit dilation to hypoxemia.** Lean and obese swine were compared during graded reductions of arterial PO<sub>2</sub> to induce hypoxemia while measuring coronary blood flow (a) and coronary resistance (b). Individual data points shown, n=6–7 per group, significance indicated by panel based on non-linear regression

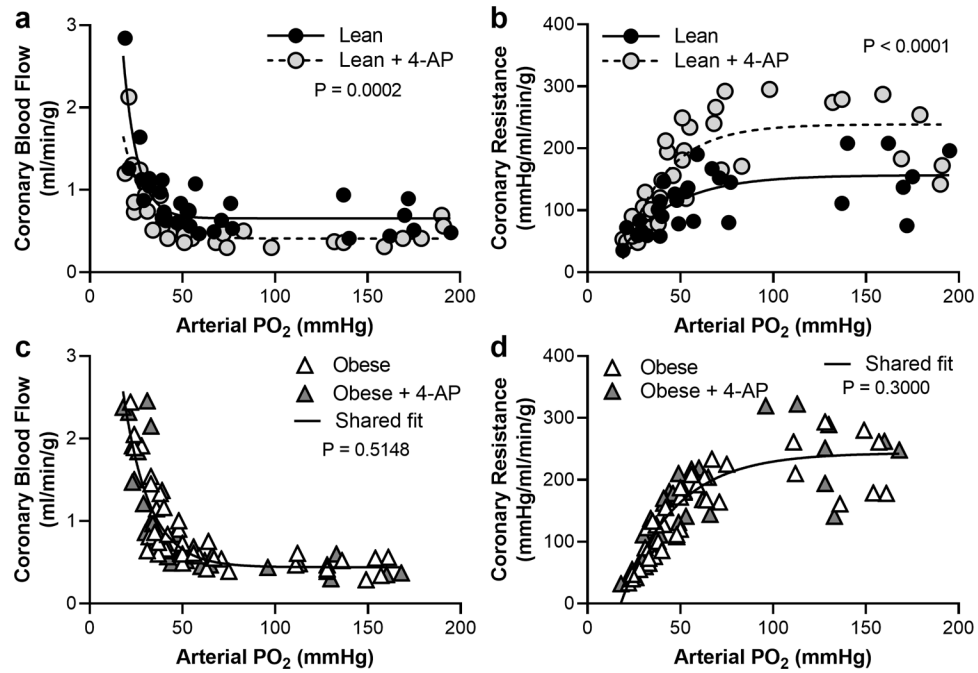


**Fig. 3.** K<sub>v</sub> blockade eliminates differences in coronary vascular resistance between lean and obese swine.

Lean (a, b) and obese (c, d) swine were exposed to graded reductions in arterial PO<sub>2</sub> to induce hypoxemia while measuring coronary blood flow (a, c) and coronary resistance (b, d) before and after acute blockade of K<sub>v</sub> channels with 4-aminopyridine (4-AP). Individual data points shown, n=6–7 per group/treatment, significance indicated by panel based on non-linear regression

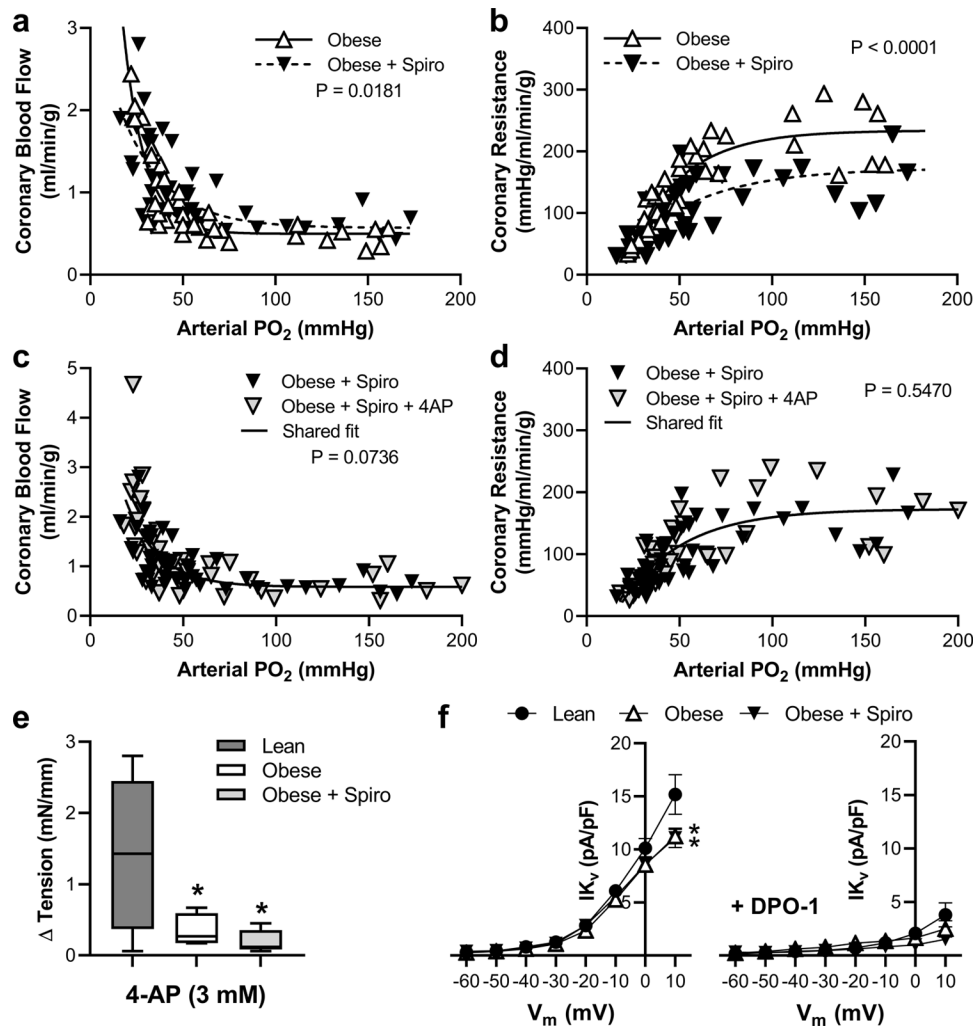


**Fig. 4. Chronic MR inhibition normalizes coronary vascular responses to graded hypoxemia in obese swine independent of  $K_v$  channels.**

Untreated obese (a, b) and spironolactone (Spiro)-treated obese (c, d) swine were exposed to graded reductions in arterial  $PO_2$  to induce hypoxemia while measuring coronary blood flow (a, c) and coronary resistance (b, d) before and after acute blockade of  $K_v$  channels with 4-aminopyridine (4-AP). *Ex vivo* constriction of isolated coronary small arteries to 4-AP was assessed in vessels from lean, obese, and spiro-treated obese swine (e). Whole cell  $K_v$  currents were measured in isolated coronary arteriolar smooth muscle cells from lean, obese, and spiro-treated obese swine in the absence and presence of the  $K_v1$  family antagonist DPO-1 (f). Individual data points (a-d) and mean  $\pm$  SE (e & f) shown,  $n=5-7$  per group/treatment (e), and  $n=32-60$  cells from 7-10 animals per group/treatment (f), significance indicated by panel based on non-linear regression (a-d), \* $p<0.05$  versus Lean (e & f)

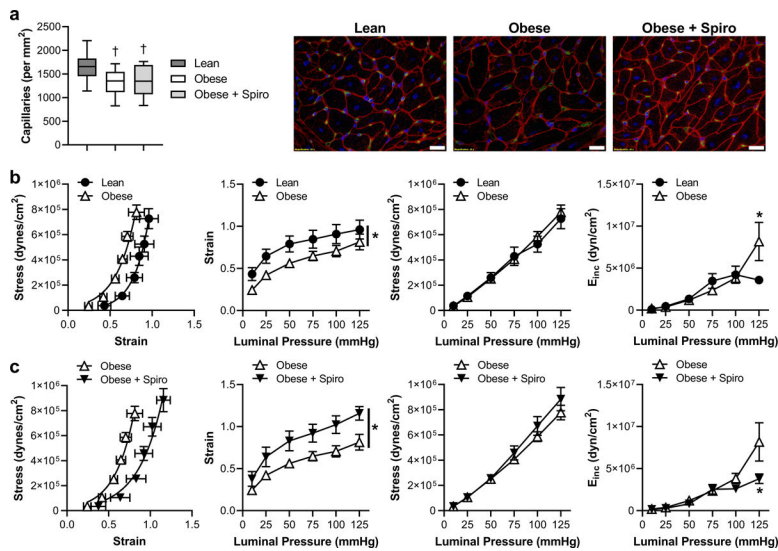


**Fig. 5. Chronic MR inhibition prevents coronary arteriolar structural stiffening in obese swine.** Cardiac capillary density was assessed in lean, obese, and spironolactone (Spiro)-treated obese swine (a). Passive coronary arteriolar stress-strain relationships and incremental modulus of elasticity were assessed in response to increasing intraluminal pressures in isolated arterioles from lean compared to obese (b) and untreated obese compared to Spiro-treated obese (c) swine. Representative capillary staining to right, scale bar = 20 $\mu$ m. Green, isolectin; Red, WGA; Blue, DAPI. Values are mean  $\pm$  SE, n=7–10; \*p<0.05, †p=0.09 versus Lean

Table 1.

Phenotype data of Ossabaw swine by treatment group

	Lean	Obese	Obese + Spiro	ANOVA
Body weight (kg)	50 ± 3	64 ± 3 <sup>*</sup>	63 ± 3 <sup>*</sup>	<i>P</i> = 0.01
Heart weight (g)	183 ± 12	190 ± 6	187 ± 6	<i>P</i> = 0.80
Heart weight/body weight ratio (g/kg)	3.7 ± 0.2	3.0 ± 0.1 <sup>*</sup>	3.0 ± 0.2 <sup>*</sup>	<i>P</i> = 0.02
Blood Glucose (mg/dl)	143 ± 6	112 ± 5 <sup>*</sup>	121 ± 7 <sup>*</sup>	<i>P</i> = 0.01
Plasma Insulin (μU/ml)	4.3 ± 1.2	3.2 ± 0.3	3.9 ± 0.7	<i>P</i> = 0.61
Total cholesterol (mg/dl)	82 ± 4	638 ± 44 <sup>*</sup>	515 ± 37 <sup>*,†</sup>	<i>P</i> < 0.001
Triglycerides (mg/dl)	53 ± 6	60 ± 7	56 ± 7	<i>P</i> = 0.79
Plasma Na <sup>+</sup> (mmol/L)	139 ± 1	138 ± 1	138 ± 1	<i>P</i> = 0.91
Plasma K <sup>+</sup> (mmol/L)	3.48 ± 0.09	3.68 ± 0.08	3.57 ± 0.09	<i>P</i> = 0.37
Plasma aldosterone (ng/dl)	62 ± 11	104 ± 15	114 ± 15	<i>P</i> = 0.06

Values are mean ± SE, n=6–10

<sup>\*</sup> *p* < 0.05 versus Lean<sup>†</sup> *p* < 0.05 versus Obese.